Impacts of Communication Limits on Convergence of Distributed DCOPF with Flexible Transmission

Qianzhi Zhang
Dept. of Electrical and Computer Engineering
University of Utah
Salt Lake City, UT, 84112
qianzhi.zhang@utah.edu

Mostafa Sahraei-Ardakani
Dept. of Electrical and Computer Engineering
University of Utah
Salt Lake City, UT, 84112
mostafa.ardakani@utah.edu

***Abstract*—**This paper presents a fully-distributed DC optimal power flow (DCOPF) method that incorporates flexible transmission, and studies the impacts of communication limitations on the convergence properties of the proposed method. The distributed DCOPF algorithm iteratively solves the first order optimality conditions at each bus. To converge to the globally optimal solution, some information is communicated to the neighboring buses. While in an ideal case such data should be communicated at each iteration, commutation limitations are an inherent characteristic of real-world implementations. This paper divides the system into different areas, and puts communication constraints between different areas. While the information between buses within the same area is communicated at each iteration, the communication between neighboring areas occurs less frequently. This paper studies the impacts of this constraint on the convergence properties of the presented distributed DCOPF algorithm. Simulation studies on IEEE 118-bus system show that communication constraints affect both the number of iterations needed to reach convergence as well as the dynamics of solution evolution.

***Index Terms*-- DC optimal power flow, distributed optimization, communication limitation, convergence, flexible transmission.**

I. Nomenclature

A. Sets and Parameters

G	Set of generators.
$G(n)$	Set of generators located at bus n.
g	Index of generators, $g \in G$.
K	Set of transmission lines not equipped with RC or PC.
k	Index of lines equipped not equipped with RC or PC, $k \in K$.
$\overline{K}$	Set of transmission lines equipped with RC.
$\overline{k}$	Index of lines equipped with RC, $\overline{k} \in \overline{K}$.
$\underline{K}$	Set of transmission lines equipped with PC.
$\underline{k}$	Index of lines equipped with PC, $\underline{k} \in \underline{K}$.
N	Set of buses.
n	Index for buses, $n \in N$.
$n(g)$	The bus at which generator g is located.
t	Index for iterations.
T	Index of iterations for information communication between two buses in different areas
$\delta^+(n)$	Set of lines specified as to bus n.
$\delta^-(n)$	Set of lines specified as from bus n.
$\delta(n)$	Set of lines connected to bus n.
a_g, b_g, c_g	Quadratic cost parameters of generator g.
B_k	Electrical susceptance of line k.
$B_{\overline{k}}$	Electrical susceptance of line $\overline{k}$ equipped with RC.
$B_{\underline{k}}$	Electrical susceptance of line $\underline{k}$ equipped with PC.
$B_{\overline{k}}^{max}, B_{\overline{k}}^{min}$	Maximum and minimum susceptance of line $\overline{k}$ equipped with RC.
F_k^{max}	Capacity of line k.
$F_{\overline{k}}^{max}$	Capacity of line $\overline{k}$ equipped with RC.
$F_{\underline{k}}^{max}$	Capacity of line $\underline{k}$ equipped with PC.
P_{L_n}	Load at bus n.
P_g^{max}, P_g^{min}	Maximum and minimum power outputs of unit g.
$z_{\overline{k}}$	Binary variable indicating the sign of voltage angle difference on line equipped with RC device.

$\theta_{\underline{k},PC}^{min}, \theta_{\underline{k},PC}^{max}$	Maximum and minimum PC voltage angle output.
$\alpha, \beta, \epsilon, \gamma, \rho$	Tuning parameters.

B. Variables

$F_{\overline{k}}$	Real power flow on line $\overline{k}$ equipped with RC.
P_g	Output of generator g.
$\theta_{k,from}, \theta_{k,to}$	Voltage angles at the "from" and "to" ends of line k.
$\theta_{\underline{k},from}, \theta_{\underline{k},to}$	Voltage angles at the "from" and "to" ends of line $\underline{k}$ equipped with PC.
$\theta_{\underline{k},PC}$	PC voltage angle set point on line $\underline{k}$ equipped with PC.
λ's	Lagrange multipliers for equality constraint x.
μ's	Lagrange multipliers for inequality constraint x.

II. Introduction

As a scalable way to handle the growing computational complexity in large-scale optimization problems, distribution optimization techniques have drawn increased attention [1]. Conventional centralized optimization in power systems requires a control center to collect all the necessary data and communicate with all the active components in the system. In distributed optimization, on the other hand, distributed control centers are just required to collect local data, solve relatively smaller problems, and communicate the information with physically connected components. Thus, local communication is an important part of distributed optimization.

There are various applications of distributed optimization in power systems. Examples include a fully distributed method to coordinate Plug-in Electric Vehicle (PEV) charging [2], and a distributed security-constrained unit commitment (SCUC) algorithm to accelerate the generation scheduling of large-scale power systems [3].

Similarly, the computational complexity of co-optimizing flexible transmission with generation dispatch [4] can also be addressed by distributed optimization. Flexible transmission can upgrade the stressed transmission system, through utilizing the existing network in a more economic and efficient way. In this paper, we present a fully distributed DC optimal power flow model which incorporates reactance controllers (RC) and voltage phase controllers (PC) [5]. Since the nonlinear model of RC flexibility will add to the computational complexity, a linear reformulation of RC flexibility [6]-[8] is applied in this paper.

Based on the different decomposition theories, distributed optimization approaches, applied in the power system operation, can be classified into different types. For example, six decomposition coordination algorithms are studied in [9], including analytical target cascading (ATC), optimality condition decomposition (OCD), alternating direction method of multipliers (ADMM), auxiliary problem principle (APP), consensus and innovations method (C+I). Reference [10] presents the C+I method to solve the DCOPF problem. This method is different from other decomposition method as it finds a distributed solution for the first order optimality condition through the distributed iterative mechanism. In this iterative structure, each bus updates a number of local variables and communicates information with its physically connected buses.

However, due to the constraints in real implementation, information communication at each iteration may be restricted. References [11]-[13] present a more realistic version of multi-level distributed approach for solving the DCOPF problem, which groups the buses into different areas, and allows information communication between buses in same area in every iteration, while information communication between buses in different areas occurs less frequently. This scheme can reduce the total communication load. In our paper, we evaluate the effect of communication limits between areas on the convergence rate of the presented distributed approach.

The contributions of this paper are summarized as follows: we first present a fully distributed DCOPF that incorporates flexible transmission with communication limitations between different areas; we, then, study the impacts of communication limitations on the convergence properties of the presented distributed approach.

The rest of the paper is organized as follows. Section III presents the modelling of the DCOPF with optimal set point adjustment of RC and PC. Section IV introduces the distributed approach of the proposed DCOPF model with limited communication. Section V shows the simulation results for IEEE 118-bus system. Section 6 concludes this work.

III. DCOPF Model with Flexible Transmission

The mathematical representation of a DCOPF with the added transmission flexibility is shown in (1)-(14). In this paper, we allow flexible transmission, in the form of reactance control and phase control, to be co-optimized with generation dispatch.

In the DCOPF formulation (1)-(8), minimizes the generation cost, while ensuring that the physical constraints of the system are not violated.

$$\min_{P_G} \sum_{n \in G} \left(a_g P_g^2 + b_g P_g + c_g\right) \tag{1}$$

$$P_g^{min} \le P_g \le P_g^{max}, \forall g \in G \tag{2}$$

$$\begin{aligned} \sum_{g \in G(n)} P_g - P_{Ln} + \sum_{k \in \delta^+(n)} F_k - \sum_{k \in \delta^-(n)} F_k + \sum_{\overline{k} \in \delta^+(n)} F_{\overline{k}} \\ - \sum_{\overline{k} \in \delta^-(n)} F_{\overline{k}} + \sum_{\underline{k} \in \delta^+(n)} F_{\underline{k}} - \sum_{\underline{k} \in \delta^-(n)} F_{\underline{k}} \\ = 0, \forall n \in N \end{aligned} \tag{3}$$

$$\theta_{slack} = 0 \tag{4}$$

$$\theta_{\underline{k},PC}^{min} \le \theta_{\underline{k},PC} \le \theta_{\underline{k},PC}^{max}, \forall \underline{k} \in \underline{K} \tag{5}$$

$$-F_k^{max} \le F_k = B_k\left(\theta_{k,from} - \theta_{k,to}\right) \le F_k^{max}, \forall k \in K \tag{6}$$

$$-F_{\overline{k}}^{max} \le F_{\overline{k}} \le F_{\overline{k}}^{max}, \forall \overline{k} \in \overline{K} \tag{7}$$

$$-F_{\underline{k}}^{max} \le F_{\underline{k}} = B_{\underline{k}}\left(\theta_{\underline{k},from} + \theta_{\underline{k},PC} - \theta_{\underline{k},to}\right) \le F_{\underline{k}}^{max}, \forall \underline{k} \in \underline{K} \tag{8}$$

The quadratic cost function is presented in (1). Generators' capacity limit constraints are modelled in (2). (3) denotes the nodal power balance constraints. The voltage angle is set to zero at the slack bus in (4). (5) denotes the PC control range. The linear flow limit constraints for transmission line sets K, $\overline{K}$ and K are represented in (6)-(8), respectively.

The linear method developed in [6]-[8] is used to eliminate the nonlinearities associated with modelling RCs. The problem represented in (9)-(14), is a mixed integer linear program that optimizes the RC set points. The binary variable, $z_{\overline{k}}$ equals to 1 when the voltage angle difference is positive. A negative voltage angle difference is being represented by $z_{\overline{k}}$ set to 0.

$$\theta_{\overline{k},from} + (1 - z_{\overline{k}})M \ge \theta_{\overline{k},to}, \forall \overline{k} \in \overline{K} \tag{9}$$

$$B_{\overline{k}}^{min}\left(\theta_{\overline{k},from} - \theta_{\overline{k},to}\right) - (1 - z_{\overline{k}})M \le F_{\overline{k}}, \forall \overline{k} \in \overline{K} \tag{10}$$

$$B_{\overline{k}}^{max}\left(\theta_{\overline{k},from} - \theta_{\overline{k},to}\right) + (1 - z_{\overline{k}})M \ge F_{\overline{k}}, \forall \overline{k} \in \overline{K} \tag{11}$$

$$\theta_{\overline{k},to} + z_{\overline{k}}M \ge \theta_{\overline{k},from}, \forall \overline{k} \in \overline{K} \tag{12}$$

$$B_{\overline{k}}^{max}\left(\theta_{\overline{k},from} - \theta_{\overline{k},to}\right) - z_{\overline{k}}M \le F_{\overline{k}}, \forall \overline{k} \in \overline{K} \tag{13}$$

$$B_{\overline{k}}^{min}\left(\theta_{\overline{k},from} - \theta_{\overline{k},to}\right) + z_{\overline{k}}M \ge F_{\overline{k}}, \forall \overline{k} \in \overline{K} \tag{14}$$

In (9)-(14), the big-M technique is used to obtain a linear formulation. The value of the binary variable $z_{\overline{k}}$, can be fixed, because the voltage angle difference can be obtained through the iterative process of the distributed optimization method.

IV. Distributed Optimization Method

The Lagrange function $\mathcal{L}$ of the DCOPF problem (1)-(14) is shown in (15). (15a) represent the partial Lagrange function for the cost function (1) and generator capacity limits (2)-(3). (15b) represents the partial Lagrange function for equality constraints (3)-(4). (15c) represents the partial Lagrange function for the inequality constraint (5). (15d) represents the partial Lagrange function for the inequality constraints (6)-(8). (15e) represents the partial Lagrange function for the inequality constraints (9)-(14).

$$\begin{aligned}\mathcal{L} = &\sum_{g\in G}\left(a_g P_g^2 + b_g P_g + c_g\right) \\ &+ \sum_{g\in G}\mu_g^+\left(P_g - P_g^{max}\right) + \sum_{g\in G}\mu_g^-\left(-P_g + P_g^{min}\right)\end{aligned} \tag{15a}$$

$$\begin{aligned}+\sum_{n=1}^{N}\lambda_n\Bigg[&-\sum_{g\in G(n)}P_g + P_{Ln} - \sum_{\overline{k}\in\delta^+(n)}F_{\overline{k}} + \sum_{\overline{k}\in\delta^-(n)}F_{\overline{k}} \\ &- \sum_{\underline{k}\in\delta^+(n)}B_{\underline{k}}\left(\theta_{\underline{k},from} + \theta_{\underline{k},PC} - \theta_{\underline{k},to}\right) \\ &+ \sum_{\underline{k}\in\delta^-(n)}B_{\underline{k}}\left(\theta_{\underline{k},from} + \theta_{\underline{k},PC} - \theta_{\underline{k},to}\right) \\ &- \sum_{k\in\delta^+(n)}B_k\left(\theta_{k,from} - \theta_{k,to}\right) \\ &+ \sum_{k\in\delta^-(n)}B_k\left(\theta_{k,from} - \theta_{k,to}\right)\Bigg]\end{aligned} \tag{15b}$$

$$\begin{aligned}&+\lambda_0\theta_{slack} \\ &+ \sum_{\underline{k}\in\underline{K}}\mu_{\underline{k},PC}^+\left(\theta_{\underline{k},PC} - \theta_{\underline{k},PC}^{max}\right) \\ &+ \sum_{\underline{k}\in\underline{K}}\mu_{\underline{k},PC}^-\left(-\theta_{\underline{k},PC} + \theta_{\underline{k},PC}^{min}\right)\end{aligned} \tag{15c}$$

$$\begin{aligned}&+\sum_{k\in K}\mu_{k,1}\left[B_k\left(\theta_{k,from} - \theta_{k,to}\right) - F_k^{max}\right] \\ &+ \sum_{k\in K}\mu_{k,0}\left[-B_k\left(\theta_{k,from} - \theta_{k,to}\right) - F_k^{max}\right] \\ &+ \sum_{\overline{k}\in\overline{K}}\mu_{\overline{k},1}\left[F_{\overline{k}} - F_{\overline{k}}^{max}\right] \\ &+ \sum_{\overline{k}\in\overline{K}}\mu_{\overline{k},0}\left[-F_{\overline{k}} - F_{\overline{k}}^{max}\right] \\ &+ \sum_{\underline{k}\in\underline{K}}\mu_{\underline{k},1}\left[B_{\underline{k}}\left(\theta_{\underline{k},from} + \theta_{\underline{k},PC} - \theta_{\underline{k},to}\right) - F_{\underline{k}}^{max}\right] \\ &+ \sum_{\underline{k}\in\underline{K}}\mu_{\underline{k},0}\left[-B_{\underline{k}}\left(\theta_{\underline{k},from} + \theta_{\underline{k},PC} - \theta_{\underline{k},to}\right) - F_{\underline{k}}^{max}\right]\end{aligned} \tag{15d}$$

$$\begin{aligned}&+z_{\overline{k}}\sum_{\overline{k}\in\overline{K}}\mu_{\bar{z},1}\left(\theta_{\overline{k},to} - \theta_{\overline{k},from}\right) \\ &+z_{\overline{k}}\sum_{\overline{k}\in\overline{K}}\mu_{\overline{RC},1}^{min}\left[-F_{\overline{k}} + B_{\overline{k}}^{min}\left(\theta_{\overline{k},from} - \theta_{\overline{k},to}\right)\right] \\ &+z_{\overline{k}}\sum_{\overline{k}\in\overline{K}}\mu_{\overline{RC},1}^{max}\left[F_{\overline{k}} - B_{\overline{k}}^{max}\left(\theta_{\overline{k},from} - \theta_{\overline{k},to}\right)\right] + \\ &+(1 - z_{\overline{k}})\sum_{\overline{k}\in\overline{K}}\mu_{\bar{z},0}\left(\theta_{\overline{k},from} - \theta_{\overline{k},to}\right) \\ &+(1 - z_{\overline{k}})\sum_{\overline{k}\in\overline{K}}\mu_{\overline{RC},0}^{max}\left[-F_{\overline{k}} + B_{\overline{k}}^{max}\left(\theta_{\overline{k},from} - \theta_{\overline{k},to}\right)\right] \\ &+(1 - z_{\overline{k}})\sum_{\overline{k}\in\overline{K}}\mu_{\overline{RC},0}^{min}\left[F_{\overline{k}} - B_{\overline{k}}^{min}\left(\theta_{\overline{k},from} - \theta_{\overline{k},to}\right)\right]\end{aligned} \tag{15e}$$

In (15), λ's and μ's represent the Lagrange multiplier for equality constraints (3)-(4) and inequality constraints (5)-(14), respectively. λ_n and λ_0 represent Locational Marginal Price (LMP) at bus n and Lagrange multiplier for voltage angle equality constraint at slack bus. μ_g^+ and μ_g^- are the Lagrange multipliers of the generator g maximum and minimum capacity inequality constraints. $\mu_{\underline{k},PC}^+$ and $\mu_{\underline{k},PC}^-$ are the Lagrange multipliers of the PC maximum and minimum control range inequality constraints. $\mu_{k,1}$, $\mu_{k,0}$, $\mu_{\overline{k},1}$, $\mu_{\overline{k},0}$, $\mu_{\underline{k},1}$ and $\mu_{\underline{k},0}$ are the Lagrange multipliers of the line flow limits on lines k, $\overline{k}$ and $\underline{k}$. $\mu_{\bar{z},1}$, $\mu_{\overline{RC},1}^{min}$ and $\mu_{\overline{RC},1}^{max}$ are Lagrange multipliers of RC flexibility with positive voltage angle difference. $\mu_{\bar{z},0}$, $\mu_{RC,0}^{min}$ and $\mu_{RC,0}^{max}$ are Lagrange multipliers of RC flexibility with negative voltage angle difference.

In the proposed model, the variables set include the variables $\left(P_g, \theta_n, F_{\bar{k}}, \theta_{\underline{k},PC}, \lambda' \text{s}, \mu' \text{s}\right)$. Based on the Lagrange function $\mathcal{L}$ in (15a)-(15e), it assumes the first order optimality KKT conditions as $\frac{\partial\mathcal{L}}{\partial P_g}, \frac{\partial\mathcal{L}}{\partial \theta_n}, \frac{\partial\mathcal{L}}{\partial F_{\bar{k}}}, \frac{\partial\mathcal{L}}{\partial \theta_{\underline{k},PC}}, \frac{\partial\mathcal{L}}{\partial \lambda_n}, \frac{\partial\mathcal{L}}{\partial \mu}$, which are used in the variable update rules.

All the iterative update rules for variables are shown in (16)-(21).

$$\lambda_n(t+1) = \lambda_n(t) - \beta\left(\frac{\partial\mathcal{L}(\mathrm{t})}{\partial\theta_n(t)}\right) + \alpha\left(\frac{\partial\mathcal{L}(\mathrm{t})}{\partial\lambda_n(t)}\right) \tag{16}$$

$$\theta_n(t+1) = \theta_n(t) - \gamma\left(\frac{\partial\mathcal{L}(\mathrm{t})}{\partial\lambda_n(t)}\right) \tag{17}$$

$$P_{g(n)}(t+1) = \mathbb{P}\left[P_{g(n)}(t) - \frac{1}{2a_{g(n)}}\left(\frac{\partial\mathcal{L}(\mathrm{t})}{\partial P_{g(n)}(t)}\right)\right] \tag{18}$$

$$F_{\bar{k}}(t+1) = \mathbb{P}\left[F_{\bar{k}}(t) - \epsilon\left(\frac{\partial\mathcal{L}(\mathrm{t})}{\partial F_{\bar{k}}(t)}\right)\right] \tag{19}$$

$$\theta_{\underline{k},PC}(t+1) = \mathbb{P}\left[\theta_{\underline{k},PC}(t) - \nu\left(\frac{\partial\mathcal{L}(\mathrm{t})}{\partial\theta_{\underline{k},PC}(t)}\right)\right] \tag{20}$$

$$\mu(t+1) = \mathbb{P}\left[\mu(t) + \rho\left(\frac{\partial\mathcal{L}(\mathrm{t})}{\partial\mu(t)}\right)\right] \tag{21}$$

where α, β, γ, ϵ, ν and ρ are positive tuning parameters. The operator $\mathbb{P}$ can project the variable value to its feasible range.

The iterative process of (16)-(21), requires communication of information between physically-connected buses. The information that needs to be communicated at bus n in every iteration t include: Locational Marginal Price $\lambda_n(t)$, voltage angle $\theta_n(t)$ and generator output $P_{g(n)}(t)$, which are associated with bus n; line flow on line $\bar{k}$ with RC devices $F_{\bar{k}}(t)$, set point of PC devices $\theta_{\underline{k},PC}(t)$, Lagrange multipliers μ's correspond line flow limit constraints and RC flexibility which are associated with the lines connected to bus n.

In the proposed iterative method, T is the iteration number, which represents the frequency of the information communication. If $T = 1$, it means that the communication of all the above variables between two buses in same area happens at every iteration. If $T > 1$, it means that the communication of all the above variables between two buses in different areas are limited to a certain number of iteration T.

V. Simulation Results

In order to evaluate the impact of the limited communication in convergence properties of the proposed distributed DCOPF model, simulation studies on IEEE 118-bus system are conducted.

PC and RC devices are installed on the more heavily congested lines in the simulations. A control range of $\pm 30\%$ for RC devices is selected in this paper, so the maximum and minimum set points of RC are calculated as (22) and (23).

$$B_{\bar{k}}^{max} = (100\% + 30\%) \times B_{\bar{k}} \tag{22}$$

$$B_{\bar{k}}^{min} = (100\% - 30\%) \times B_{\bar{k}} \tag{23}$$

From (9)-(14), the RC flexible model directly optimizes the $F_{\bar{k}}$ line flow on line $\bar{k}$ with RC device, instead of directly optimizing the RC device set point. Therefore, based on DC power flow equation, the set point of RC device can be calculated as shown in (24) and (25).

$$B_{\bar{k}}^{RC} = \frac{F_{\bar{k}}}{\theta_{\bar{k},from} - \theta_{\bar{k},to}} \tag{24}$$

$$\text{RC set point} = \left(\frac{B_{\bar{k}}^{RC} - B_{\bar{k}}}{B_{\bar{k}}}\right)\% \tag{25}$$

The PC devices has a control range of ± 0.1 rad, which means $\theta_{\underline{k},PC}^{min} = -0.1$ rad and $\theta_{\underline{k},PC}^{max} = 0.1$ rad. The PC set point $\theta_{\underline{k},PC}$ is directly optimized in the proposed model.

Data for IEEE 118-bus is taken from [14], which consists of 19 generators, 180 branches and 99 demand nodes. In the simulations, the system is separated into three subareas, which is shown in Fig.1.

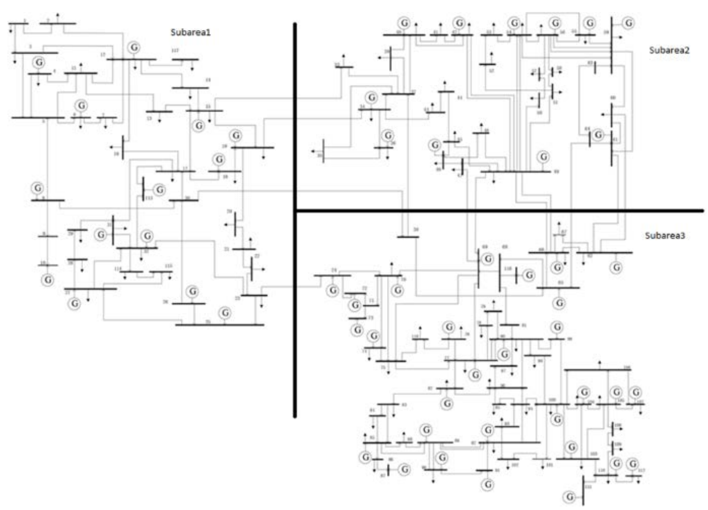

Fig. 1. IEEE 118-bus System in Three Areas

The result from a conventional DCOPF (has no RC or PC devices) shows that there are three congested lines: two heavily congested lines from Bus 77 to Bus 82 and Bus 89 to Bus 92, and one lightly congested line from Bus 65 to Bus 68. The total system cost is $78,412 when there are no RC or PC devices in the system

In order to test the convergence properties of the developed model, the worst-case scenario of a cold-start is simulated here, where the solver does not have any initial guess. In a cold start, all generation outputs, bus angles and the Lagrange multipliers μs are set to zero at the start of the simulation. The LMPs, λ_n, are set to an initial value of 25 $/MWh.

Two cases are studied in this section. In Case 1, the communication between two connected buses in different areas happens in every iteration, which means $T = 1$. In Case 2, the communication between two connected buses in different areas happens every 20 iterations, which translates to $T = 20$.

In both cases, one RC and one PC are installed on the congested lines connecting Bus 77 to Bus 82 and Bus 89 to Bus 92 respectively. For both simulations, the tuning parameters are set the values given in Tab.1.

TABLE 1
Tuning Parameter Values for Case 1-2

Tuning Parameters	Case 1,2
α	0.1485
β	0.0019
ϵ	0.0001
γ	0.0017
ρ	0.16

From Fig.2 to Fig.5, the optimal results from distributed DCOPF for Case 1 and Case 2 are shown.

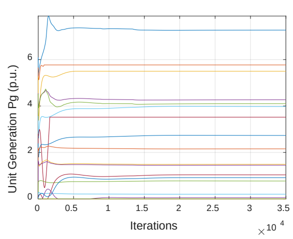

Fig. 2.1 Case1-Unit Generation Outputs (P_g)

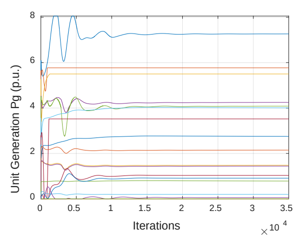

Fig. 2.2 Case 2- Unit Generation Outputs (P_g)

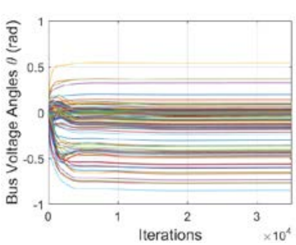

Fig. 3.1 Case 1-Bus Voltage Angles (θ_n)

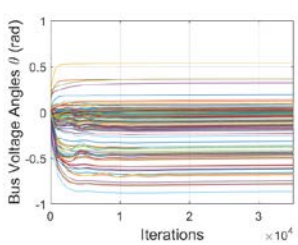

Fig. 3.2 Case 2-Bus Voltage Angles (θ_n)

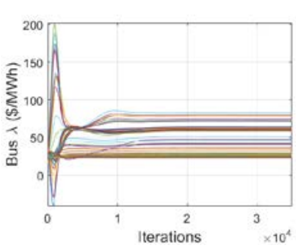

Fig. 4.1 Case1-Bus LMPC (λ_n)

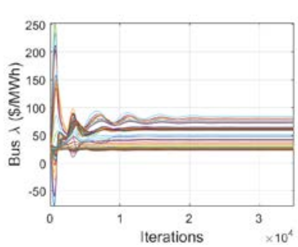

Fig. 4.2 Case2-Bus LMPC (λ_n)

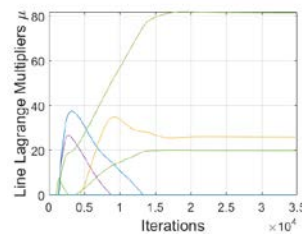

Fig. 5.1 Case 1-Line Lagrange Multipliers (μ)

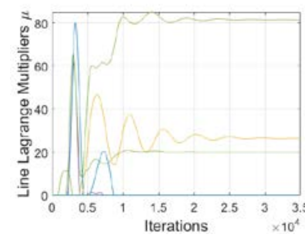

Fig. 5.2 Case 2-Line Lagrange Multipliers (μ)

Based on (24) and (25), in Case 1 and Case 2, the RC and PC set points are 18.6% and -0.1 rad. The total operation cost is $72,260, with a total cost saving of 7.87%.

From the comparisons between Case 1 and Case 2 through Fig. 2 to Fig. 5, we can observe that even through the results from those two cases are very similar, which the average differences are less than 1%, the oscillation due to the limited communications in Case 2 has the negative impact to the convergence properties of the proposed distributed DCOPF model.

In order to better evaluate the performance of Case 1 and Case 2, the relative distance of the objective function from the optimal value over the iterations is calculated, which is given in (26):

$$rel = \frac{|f - f^*|}{f^*} \tag{26}$$

where f^* is the optimal objective function value calculated by solving Case 1 with full communication. And f is the objective function value in each iteration from Case 1 or Case 2. In Fig. 6 presents the *log* values of *rel* when $T = 1, 5, 15, 20$, repesctively.

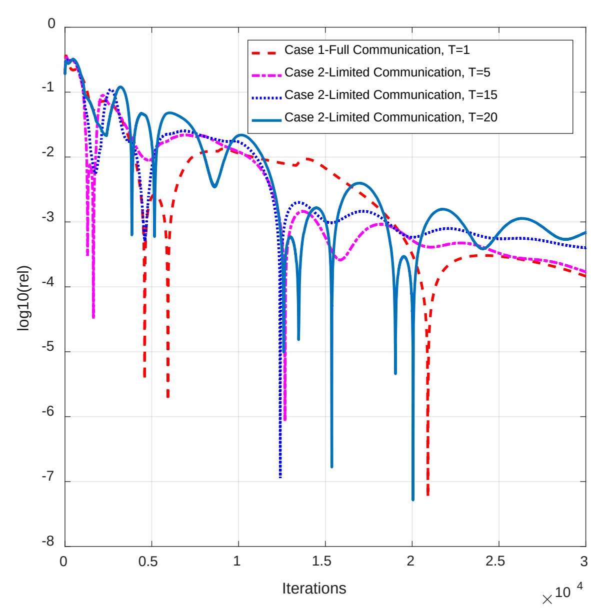

Fig. 6. Relative Distance to Solution $\ln(\frac{|f-f^*|}{f^*})$

Fig. 6 shows that when T is chosen to be larger, the method shows stronger oscillations and the convergence rate will be slower. However, the oscillations and convergence is not very sensitive to T. While Fig. 6 is one indicator of the convergence, it should be noted that the feasibility is another issue, which is not necessarily reflected in Fig. 6. Specially, the curves in Fig. 6 show serval dips, that are infeasible solutions during the iterative process.

V. Conclusions

In this paper, we study the impacts of communication limitations on the convergence properties of the presented distributed DCOPF algorithm. The method co-optimizes generation dispatch and the set points of reactance and phase controllers.

The simulation results from IEEE 118-bus system reveal that: (1) communication limitations will lead to oscillations in the iterative update process and reduce the convergence rate of the presented distributed method. However, the impact may be limited. (2) The optimal results from the presented method with different communication limitation frequencies T are relatively close to each other. (3) There is a trade-off between the convergence rate and the overall communication load. With a reasonable value of T, the overall communication load can be reduced while the convergence rate is ensured to be in an acceptable range.

References

[1] Wang Y, Wang S, Wu L. “Distributed optimization approaches for emerging power systems operation: A review,” *Electric Power Systems Research*, vol.144, pp. 127-135, March 2017.

[2] J. Mohammadi, G. Hug, S. Kar, "A Fully Distributed Cooperative Charging Approach for Plug-in Electric Vehicles," *IEEE Trans. on Smart Grid*, early access.

[3] A. Kargarian, Y. Fu and Z. Li, "Distributed Security-Constrained Unit Commitment for Large-Scale Power Systems," *IEEE Trans. Power Syst*, vol. 30, no. 4, pp. 1925-1936, July 2015.

[4] J. D. Lyon *et al*., "Harnessing Flexible Transmission: Corrective Transmission Switching for ISO-NE," *IEEE Power and Energy Technology Systems Journal*, vol. 3, no. 3, pp. 109-118, Sept. 2016.

[5] K. Baker, J. Guo, G. Hug and X. Li, "Distributed MPC for Efficient Coordination of Storage and Renewable Energy Sources Across Control Areas," *IEEE Trans. on Smart Grid*, vol. 7, no. 2, pp. 992-1001, March 2016.

[6] M. Sahraei-Ardakani and K. W. Hedman, "A Fast LP Approach for Enhanced Utilization of Variable Impedance Based FACTS Devices," *IEEE Trans. Power Syst*, vol. 31, no. 3, pp. 2204-2213, May 2016.

[7] M. Sahraei-Ardakani and K. W. Hedman, "Day-Ahead Corrective Adjustment of FACTS Reactance: A Linear Programming Approach," *IEEE Trans. Power Syst*, vol. 31, no. 4, pp. 2867-2875, July 2016.

[8] M. Sahraei-Ardakani and K. W. Hedman, "Computationally Efficient Adjustment of FACTS Set Points in DC Optimal Power Flow With Shift Factor Structure,” *IEEE Trans. Power Syst*, vol. 32, no. 3, pp. 1733-1740, May 2017.

[9] A. Kargarian; J. Mohammadi; J. Guo; S. Chakrabarti; M. Barati; G. Hug; S. Kar; R. Baldick, "Toward Distributed/Decentralized DC Optimal Power Flow Implementation in Future Electric Power Systems," *IEEE Trans. on Smart Grid*, early access.

[10] J. Mohammadi, G, Hug, and S. Kar, “Distributed approach for DC optimal power flow calculation,” Dept. Electr. Eng., Carnegie Mellon Univ., 2014. [Online]. Available: https://arxiv.org/pdf/1410.4236v1.pdf

[11] J. Mohammadi, J. Zhang, S. Kar, G. Hug and J. M. F. Moura, "Multilevel distributed approach for DC Optimal Power Flow," *in Proc.2015 IEEE Global Conference on Signal and Information Processing (GlobalSIP)*, Orlando, FL, pp. 1121-1125, Dec. 2015.

[12] J. Mohammadi, G. Hug and S. Kar, "Asynchronous distributed approach for DC Optimal Power Flow," *in Proc.2015 IEEE Eindhoven PowerTech*, Eindhoven, pp. 1-6, July 2015.

[13] J. Guo, G. Hug and O. K. Tonguz, "Intelligent Partitioning in Distributed Optimization of Electric Power Systems," in *IEEE Transactions on Smart Grid*, vol. 7, no. 3, pp. 1249-1258, May 2016.

[14] Power System Test Case Archive, Dept. Electr. Eng., Univ. Washington, Seattle, WA, USA, 2007. [Online]. Available: http://www2.ee.washington.edu/research